scientific reports

Check for updates

OPEN

Laser cooling with intermediate state of spin–orbit coupling of LuF molecule

N. El-Kork[1,2]✉, A. AlMasri Alwan[1], N. Abu El Kher[1,5], J. Assaf[3,4], T. Ayari[1], E. Alhseinat[1] & M. Korek[5]

This work presents a theoretical study of the laser cooling feasibility of the molecule LuF, in the fine structure level of approximation. An ab-initio complete active space self-consistent field (CASSCF)/MRCI with Davidson correction calculation has been done in the $\Lambda^{(\pm)}$ and $\Omega^{(\pm)}$ representations. The corresponding adiabatic potential energy curves and spectroscopic parameters have been investigated for the low-lying electronic states. The calculated values of the internuclear distances of the $X^3\Sigma_{0+}$ and $(1)^3\Pi_{0+}$ states show the candidacy of the molecule LuF for direct laser cooling. Since the existence of the intermediate $(1)^3\Delta_1$ state cannot be ignored, the investigation has been done by taking into consideration the two transitions $(1)^3\Pi_{0+}$–$(1)^3\Delta_1$ and $(1)^3\Pi_{0+}$ –$X^3\Sigma_{0+}$. The calculation of the Franck–Condon factors, the radiative lifetimes, the total branching ratio, the slowing distance, and the laser cooling scheme study prove that the molecule LuF is a good candidate for Doppler laser cooling.

Cold and ultracold molecules offer new insights into many-body physics, revolutionize physical chemistry, and provide techniques for probing new states of quantum matter. They represent an exciting new frontier that enables the investigation of measurements at an unprecedented level of detail. Besides, polar ultracold molecules present new platforms for quantum information, quantum computing[1–4], and quantum simulation of many-body interactions[5,6]. Dipole–dipole interactions among ultracold polar molecules, such as LuF can lead to discoveries beyond traditional molecular science[7].

The group of lutetium mono-halides LuX (X = F, Cl, Br, I) has been the subject of numerous experimental and theoretical studies and has an increasing interest in various types of research[8–11]. LuF is an element of the lutetium mono-halides LuX group, which is significant in astrophysics due to their presence in many stars enriched by the r-nucleosynthesis process[12–15], in the interstellar medium[16], and in the cool stellar atmospheres[17]. This molecule has been studied experimentally in literature[18–21], while the theoretical studies in $\Lambda^{(\pm)}$ representation are given in Refs.[22–28]. The $\Omega^{(\pm)}$ states of LuF molecules have been investigated by Assaf et al.[29], where 36 electronic states have been investigated.

Computation and results

We initially performed preliminary investigations of the electronic structure of the LuF molecule in the spin-free approximation. The Quantum Chemistry Package Molpro 2010[30] was used by applying the *ab-initio* Complete Active Space Self-consistent field (CASSCF) method. The adiabatic potential energy curves have been calculated by employing the internally contracted Multi Reference Configuration interaction plus Davidson correction (MRCI + Q) techniques within the Born–Oppenheimer approximation. In the $\Lambda^{(\pm)}$ representation, the adopted basis sets for the Lu and F atoms are respectively ECP60MWB (using *s*, *p*, *d* atomic orbitals) and ECP2SDF (using *s*, *p* atomic orbitals). The investigated potential energy curves in this representation for the lower electronic states are shown in Fig. 1. We can note that the first low-lying states of the LuF molecule are of triplet multiplicity as in all electronic structures reported previously[27–29]. The spectroscopic constants T_e, R_e, ω_e, $\omega_e x_e$, B_e, α_e, and D_e have been calculated by fitting the potential energy curve values around the minimum of the internuclear distance R_e to a polynomial in terms of R, the significant degree of which is determined from the evaluation of the statistical error for the coefficients, for the ground and the low-lying states of the LuF molecule, as presented in Table 1. In this Table, the comparison of our calculated value of R_e for the ground and the investigated excited

[1]Department of Physics, Khalifa University, P.O. Box 57, Abu Dhabi, United Arab Emirates. [2]Space and Planetary Science Centre, Khalifa University, Abu Dhabi, United Arab Emirates. [3]Doctoral School of Sciences and Technology, Lebanese University, Hadath, Lebanon. [4]Center for Educational Research and Development, CERD, Sin El Fil, Lebanon. [5]Faculty of Science, Beirut Arab University, Riad El Solh, Beirut 1107 2809, Lebanon. ✉email: nayla.elkork@ku.ac.ae

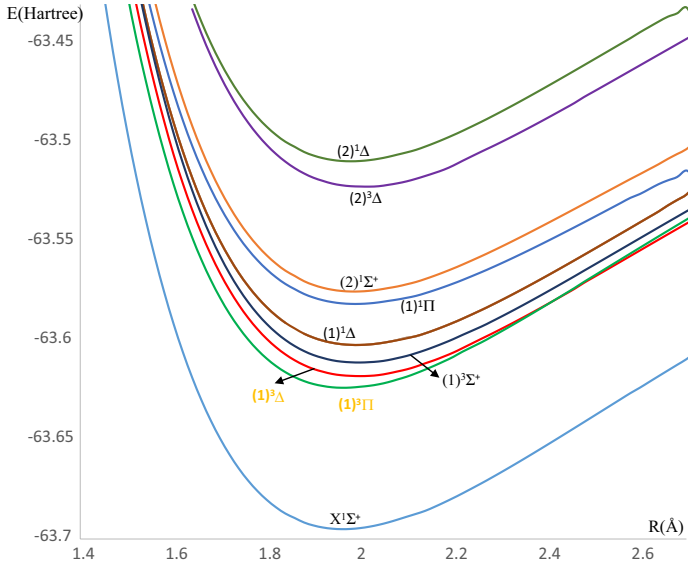

Figure 1. The potential energy curves of the low-lying free spin singlet and triplet electronic states of LuF molecule.

States	Ref.	R_e (Å)	$\Delta R_e/R_e$ %	T_e (cm^{-1})	$\Delta T_e/T_e$ %	ω_e (cm^{-1})	$\Delta\omega_e/\omega_e$ %	$\omega_e x_e$ (cm^{-1})	$\Delta\omega_e x_e/\omega_e x_e$ %	B_e (cm^{-1})	$\Delta B_e/B_e$ %	$\alpha_e \times 10^3$ (cm^{-1})	$D_e \times 10^6$ (cm^{-1})
$X^1\Sigma^+$	Present work	1.962		0		614.15		2.60		0.256		1.55	0.181
	a	1.922	*2.0*	0	*0.0*	606.6	*1.2*	3.30	*21.2*	–		–	–
	b	1.918	*2.2*	0	*0.0*	612.91	*0.2*	2.52	*3.1*	–		–	–
	c	1.913	*2.5*	0	*0.00*	618.89	*0.8*	2.53	*2.7*	–		–	–
	d	–		–		**610.6**	***0.6***	**2.5**	***3.8***	–		–	–
	e	**1.9165**	***2.3***	**0**	***0.0***	**611.79**	***0.4***	**2.54**	***2.3***	**0.268**	***4.5***	**1.56**	**0.205**
	f	**1.917**	***2.3***	–		**618**	***0.6***	**2.82**	***7.8***	**–**		**–**	**–**
$(1)^3\Pi$	Present work	1.967		15 684		576.95		2.33		0.254		1.685	0.197
	a	1.923	*2.2*	16 165	*3.0*	596.2	*3.2*	3.0	*22.3*	–		–	–
	b	1.928	*2.0*	16 602	*5.5*	590.96	*2.4*	2.66	*12.4*	–		–	–
	c	1.933	*1.7*	15 956	*1.7*	579.22	*0.4*	2.67	*12.7*	–		–	–
$(1)^3\Delta$	Present work	1.997		16 962		551.68		3.0		0.247		0.815	0.207
	a	1.952	*2.3*	17 904	*5.3*	561.00	*1.7*	3.40	*11.8*	–		–	–
	b	1.946	*2.6*	16 653	*1.8*	572.9	*3.7*	3.52	*14.8*	–		–	–
	c	1.947	*2.5*	14 927	*12.0*	576.04	*4.2*	2.71	*9.7*	–		–	–
$(1)^3\Sigma^+$	Present work	1.997		18 484		548.33		2.73		0.247			
	a	1.953	2.2	19 131	*3.4*	567.1	*3.3*	2.6	*4.8*	–		–	–
	b	1.955	2.1	19 296	*4.2*	570.22	*3.8*	2.6	*4.8*	–		–	–
	c	1.961	1.8	18 856	*2.0*	559.57	*2.0*	2.50	*8.4*	–		–	–
$(1)^1\Delta$	Present work	1.992		20 428		567.43		2.55		0.248		2.24	0.189
	a	1.956	*1.8*	21 634	*5.6*	555.0	*2.2*	2.5	*2.0*	–		–	–
	b	1.952	*2.0*	21 137	*3.4*	568.99	*0.3*	2.57	*0.8*	–		–	–
	c	1.955	*1.9*	19 471	*4.7*	567.71	*0.0*	2.81	*9.3*	–		–	–
$(1)^1\Pi$	Present work	1.988		24 973		544.28		2.57		0.249		2.35	0.221
	a	1.945	*2.2*	25 538	*2.2*	544.7	*0.1*	2.6	*1.2*	–		–	–
	b	1.958	*1.5*	24 633	*1.4*	540.48	*0.7*	2.22	*13.6*	–		–	–
	c	1.972	*0.8*	23 708	*5.1*	525.34	*3.5*	2.18	*15.2*	–		–	–
	d	–		–		**542.6**	***0.3***	**2.3**	***10.5***	–		–	–
	e	**1.958**	***1.5***	**24 465.68**	***2.0***	**543.42**	***0.2***	**2.28**	***11.3***	**0.256**	***2.7***	**1.61**	**0.228**

Table 1. The spectroscopic constants of the spin-free $^{2s+1}\Lambda^{(+/-)}$ electronic states of LuF molecule. Percentage relative error values are in [italics]. [a]Ref. [27], [b]Ref. [28], [c]Ref. [29], [d]Ref. [18], [e]Ref. [19,20], [f]Ref. [21]. Experimental values are indicated in bold.

electronic states with those given in the literature proved a suitable accuracy with relative difference values that are less than 3%.

Similarly, the values of T_e and ω_e also present a good agreement for the six studied states with relative differences close to 12% compared with the literature. Comparing our values with the experimental data[18–21] for the ground state proves a high accuracy with average percentage errors of 4.6%, 4.5%, 0.6%, and 11.7% for $\omega_e x_e$, B_e, α_e, and D_e respectively. Furthermore, the electronic spectrum of the LuF molecule has been recorded experimentally using a hollow cathode lamp by D'Incan et al.[18] and Effantin et al.[19]; they assigned the following notation for the excited states : $A^1\Sigma^+$, $B^1\Pi$, $D^1\Pi$, $E^1\Pi$, and $F^1\Sigma^+$. However, similarly to Assaf et al.[29] and Hamadeh et al.[27], in our work, the first excited state was found to be a $^1\Pi$ state, with a transition energy $T_e = 24\,973\ cm^{-1}$. This state doesn't correspond to the observed A, B, or D systems, but to the reported $E^1\Pi$ state, where the spectroscopic constants average relative differences with our calculations are 2.0% for Te, 1.5% for Re, 0.3% for ω_e and 2.7% for Be.

We perform our calculations with Spin–Orbit Coupling (S.O.C) effects for the LuF molecule in the $\Omega^{(\pm)}$ representation for a more accurate description of experimentally observed systems. We use the same basis sets ECP28-MWB with ANO-SO[31] for the Lu atom and an all-electrons scheme for the F atom[32] as presented by Assaf et al.[29]. The potential energy curves and the splitting energies for the three lowest electronic states $X^1\Sigma^+$ ($X^1\Sigma_{0+}$), $(1)^3\Pi$ ($(1)^3\Pi_{0+}$, $^3\Pi_{0-}$), and $(1)^3\Delta$ ($(1)^3\Delta_1$, $(1)^3\Delta_2$) are respectively given in Figs. 2 and 3. Also, the accurate spectroscopic constants of the bound Ω states of LuF molecule have been calculated and listed in Table 2 with the same method used for the spin-free states. As shown in Figs. 2 and 3, we find relatively large values of the splitting energies for $^3\Pi$ (about 375 cm^{-1}) and $^3\Delta$ states (about 930 cm^{-1}) indicating the significant effects of the spin–orbit coupling on the electronic states of the LuF molecule. Effantin et al. observed five bands for singlet transition systems: $A^1\Sigma^+ \rightarrow X^1\Sigma^+$, $B^1\Pi \rightarrow X^1\Sigma^+$, $D^1\Pi \rightarrow X^1\Sigma^+$, $E^1\Pi \rightarrow X^1\Sigma^+$, and $F^1\Sigma^+ \rightarrow X^1\Sigma^+$. As discussed by Hamade et al.[27] a comparison of the observed levels with those obtained throught our calculations, shows that the upper states A and B are not equivalent to any $^1\Sigma^+$ and $^1\Pi$. Rather, the transition $A^1\Sigma^+ \rightarrow X^1\Sigma^+$ predicted by Effantin et al. shows a band of $\Delta\Omega = 0$, which is attributed to the spin–orbit transition $^3\Pi_{0+} \rightarrow X^1\Sigma_{0+}$. On other hand, the observed transition $B^1\Sigma^+ \rightarrow X^1\Sigma^+$ transition of $\Delta\Omega = 1$, is equivalent to that of $^3\Pi_1 \rightarrow X^1\Sigma_{0+}$. These results led us to confirm that the upper states $A^1\Sigma^+$ and $B^1\Pi$ are the components $^3\Pi_{0+}$ and $^3\Pi_1$ of $(1)^3\Pi$ state respectively. Consequently, our calculations show a good agreement with the experiment conducted by Effantin et al. for the $(1)^3\Pi_{0+}$ state with a relative discrepancy $\Delta R_e/R_e = 0.2\%$, $\Delta T_e/T_e = 7.2\%$, $\Delta\omega_e/\omega_e = 0.5\%$, $\Delta\omega_e x_e/\omega_e x_e = 4.6\%$, and $\Delta B_e/B_e = 0.4\%$.

We also performed a rovibrational study of the investigated states using the canonical function approach[33–35] and cubic spline interpolation between every two consecutive points of the potential energy curves. Table 3 shows the vibrational energy Ev, the rotational constant B_v, and the centrifugal distortion constant D_v for the investigated spin-free ($\Lambda^{(\pm)}$ representation) and spin–orbit ($\Omega^{(\pm)}$ representation) curves, with a comparison with previously published data. Our values for the different vibrational levels of the $(X)^1\Sigma^+$, $(1)^1\Pi$, $X^1\Sigma_{0+}$, and $(1)^3\Pi_{0+}$ states of LuF molecule agree well with the experimental ones[19,21,22], with an relative difference of

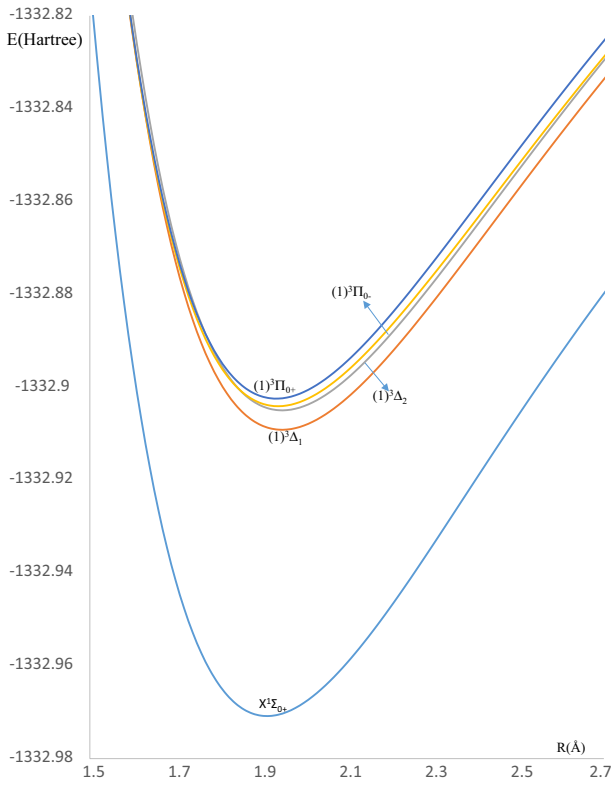

Figure 2. The potential energy curves of the low-lying spin orbit states of LuF molecule.

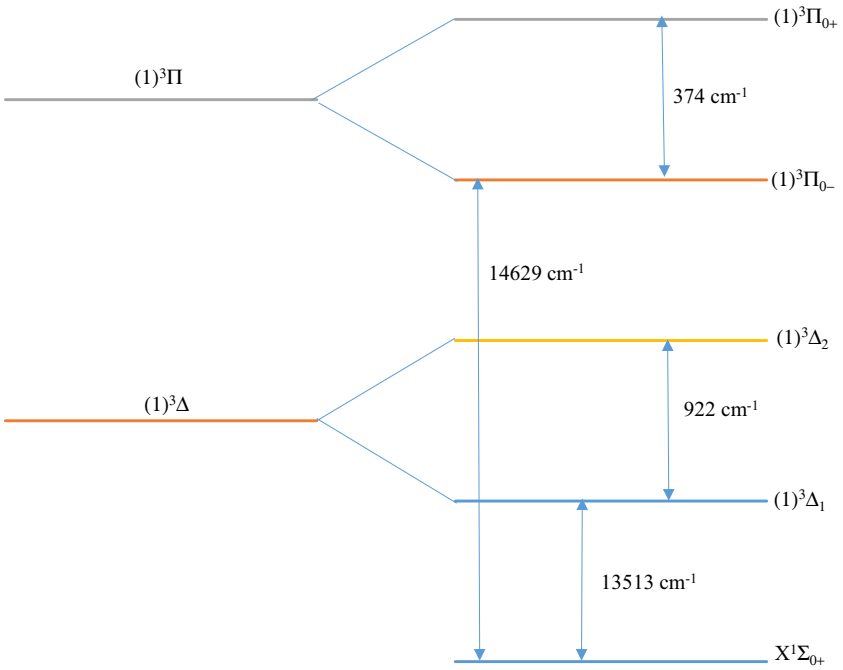

Figure 3. Values of the splitting energy of $^3\Pi$ and $^3\Delta$ of the molecule LuF.

States	Ref.	R_e (Å)	$\Delta R_e/R_e$ %	T_e (cm^{-1})	$\Delta T_e/T_e$ %	ω_e (cm^{-1})	$\Delta\omega_e/\omega_e$ %	$\omega_e x_e$ (cm^{-1})	$\Delta\omega_e x_e/\omega_e x_e$ %	B_e (cm^{-1})	$\Delta B_e/B_e$ %	$\alpha_e\times10^3$ (cm^{-1})	$D_e\times10^6$ (cm^{-1})
$X^1\Sigma_{0+}$	Present work	1.914		0		618.93		2.77		0.268		1.62	0.202
	a	1.914	*0.0*	0	*0.0*	619.36	*0.1*	2.53	*8.7*	–		–	–
	b	–		–		**610.6**	***1.3***	**2.5**	***9.7***	–		–	–
	c	**1.9165**	***0.13***	**0**	***0.0***	**611.79**	***1.2***	**2.54**	***8.3***	**0.268**	***0.0***	**1.56**	**0.205**
$(1)^3\Delta_1$	Present work	1.949		13 534.68		572.75		2.54		0.259		1.55	0.212
	a	1.949	*0.0*	13 513	*0.16*	572.44	*0.1*	2.57	*1.2*	–		–	–
$(1)^3\Delta_2$	Present work	1.949		14,453.39		572.29		2.56		0.259		1.55	0.212
	a	1.949	*0.0*	14 435	*0.1*	572.74	*0.1*	2.82	*9.2*	–		–	–
$(1)^3\Pi_{0-}$	Present work	1.939		14 645.20		571.81		2.86		0.261		1.61	0.219
	a	1.938	*0.1*	14 629	*0.1*	573.32	*0.3*	2.58	9.8	–		–	–
$(1)^3\Pi_{0+}$	Present work	1.935		15 007.58		585.13		2.47		0.263		1.59	0.218
	a	1.935	*0.0*	15 003	*0.0*	577.29	*1.3*	2.69	*8.2*	–		–	–
	b	–		–		**586.4**	***0.2***	**2.5**	***1.2***	–		–	–
	c	**1.9313**	***0.2***	**16 164.64**	***7.2***	**587.95**	***0.5***	**2.59**	***4.6***	**0.264**	***0.4***	**1.62**	**0.208**

Table 2. The spectroscopic constants of the spin–orbit $\Omega^{(\pm)}$ electronic states of LuF molecule. Percentage relative error values are in [italics]. [a]Ref. [29], [b]Ref. [18], [c]Ref. [19,20]. Experimental values are indicated in bold.

$0.3\% \leq \Delta E_v/E_v \leq 2.6\%$, $0.3\% \leq \Delta B_v/B_v \leq 5.1\%$, and $0\% \leq \Delta D_v/D_v \leq 21.5\%$. We compared in Table 3 the ro-vibrational constants values for $X^1\Sigma^+$ that were reported by Effantin et al.[19] with our calculated $X^1\Sigma^+$ and $X^1\Sigma_{0+}$ values to confirm that this state is of $X^1\Sigma_{0+}$ nature. In fact, the values of B_v and D_v of $X^1\Sigma_{0+}$ are closer to experimental data than those for $X^1\Sigma^+$, as previously discussed. Generally, our present calculations agree with the available experimental values, which confirms the credibility of our work. In addition, Table 4 shows the ro-vibrational constant values for the remaining low-lying excited states of the LuF molecule. No comparison has been reported for these levels since they are given here for the first time.

To further verify the truthfulness of our data, we calculated the wavenumbers of the rotational components for P-branch and R-branch for $(1)^3\Pi_{0+}-X^1\Sigma_{0+}$ system as listed in Table 5 by applying the concept of Loomis-Wood diagrams for linear molecules[36]. This method is based on expressing the rovibrational transitions for the P-branch and R-branch as a polynomial of fourth degree in m with $m = -J$ for the P-branch and $m = J + 1$ for the R-branch using the following relation:

State	v	E_v (cm^{-1})	$\Delta E_v/E_v$ %	B_v (cm^{-1})	$\Delta B_v/B_v$ %	$D_v \times 10^7$ (cm^{-1})	$\Delta D_v/D_v$ %
$(X)^1\Sigma^+$	0	306.09 – – 305.24[c]	***0.3***	0.2544 **0.2669**[a] **0.2669**[b] –	***4.7*** ***4.7***	1.82 **2.02**[a] – –	***9.9***
	1	905.94 – – 911.91[c]	***0.7***	0.2529 **0.2653**[a] **0.2653**[b] –	***4.7*** ***4.7***	1.85 **2.03**[a] – –	***8.9***
	2	1497.36 1513.50[c]	***1.1***	0.2509 **0.2638**[a] **0.2637**[b] –	***4.9*** ***4.9***	2.02 **2.07**[a] – –	***2.4***
	3	2072.44 2110.01[c]	***1.8***	0.2489 **0.2622**[a] –	***5.1***	2.13 **2.03**[a] –	***4.7***
	4	2634.09 – 2701.45[c]	***2.5***	0.2479 **0.2606**[a] –	***4.9***	1.70 **2.15**[a] –	***20.9***
	5	3201.05 3287.80[c]	***2.6***	0.2474 –		1.52 –	
	6	3774.33 3869.08[c]	***2.4***	0.2458 –		1.79 –	
	7	4343.23 4445.28[c]	***2.3***	0.2441 –		1.85 –	
	8	4908.06 5016.39[c]	***2.2***	0.2433 –		1.94 –	
	9	5468.05 5582.43[c]	***2.0***	0.2422 –		1.81 –	
	10	6024.00 6143.39[c]	***1.9***	0.2405 –		1.55 –	
	11	6579.43 6699.26[c]	***1.8***	0.2393 –		1.89 –	
	12	7129.85 7250.06[c]	***1.7***	0.2381 –		1.90 –	
	13	7675.59 7795.77[c]	***1.5***	0.2369 –		1.74 –	
	14	8218.25 8336.40[c]	***1.4***	0.2355 -		1.72 -	
	15	8757.58		0.2342		1.73	
	16	9293.71		0.2330		1.90	
	17	9825.33		0.2318		1.80	
	18	10,353.34		0.2306		1.75	
	19	10,877.89		0.2293		1.78	
	20	11,398.89		0.2281		1.85	
	21	11,915.89		0.2270		1.76	
	22	12,429.47		0.2257		1.75	
	23	12,939.64		0.2245		1.77	
	24	13,446.27		0.2233		1.75	
	25	13,949.48		0.2221		1.78	
	26	14,449.10		0.2209		1.80	
	27	14,944.97		0.2197		1.84	
	28	15,436.68		0.2183		1.88	
	29	15,923.88		0.2170		1.90	
	30	16,406.59		0.2157		1.77	
	31	16,885.95		0.2147		1.53	
	32	17,363.70		0.2138		1.55	
	33	17,839.58		0.2127		1.85	
	34	18,311.45		0.2114		1.88	
	35	18,779.22		0.2103		1.45	
	36	19,245.77		0.2097		1.35	
	37	19,711.75		0.2088		1.63	
	38	20,175.42		0.2079		1.54	
	39	20,637.04		0.2070		1.65	
	40	21,095.66		0.2056		2.23	

Continued

State	v	E_v (cm^{-1})	$\Delta E_v/E_v$ %	B_v (cm^{-1})	$\Delta B_v/B_v$ %	$D_v \times 10^7$ (cm^{-1})	$\Delta D_v/D_v$ %
	41	21,547.86		0.2038		2.03	
	42	21,994.96		0.2028		1.44	
	43	22,440.43		0.2020		1.48	
	44	22,884.18		0.2010		1.67	
	45	23,325.08		0.1999		1.82	
	46	23,762.34		0.1988		1.54	
	47	24,197.39		0.1980		1.45	
	48	24,630.69		0.1970		1.70	
	49	25,061.06		0.4071		39.34	
	50	25,489.11		0.4057		53.98	
	51	25,915.13		0.4037		74.36	
	52	26,339.00		0.4009		101.72	
	53	26,760.48		0.3883		98.08	
	54	27,180.01		0.3850		104.46	
	55	27,597.29		0.3874		401.55	
	56	28,011.78		0.4311		14.87	
	57	28,423.21		0.4305		23.68	
	58	28,829.96		0.4298		34.53	
	59	29,231.13		0.4288		48.13	
	60	29,626.79		0.4276		58.21	
	61	30,018.94		0.4254		93.97	
	62	30,409.89		0.4232		114.06	
	63	30,798.70		0.4203		134.71	
	64	31,183.37		0.4165		152.06	
	65	31,564.11		0.4117		161.84	
	66	31,943.20		0.4042		211.34	
	67	32,319.77		0.4432		3.09	
	68	32,692.66		0.4430		4.75	
	69	33,063.28		0.4426		4.24	
	70	33,431.98		0.4422		2.18	
	71	33,797.67		0.4416		2.90	
State	v	E_v (cm^{-1})	$\Delta E_v/E_v$ %	B_v (cm^{-1})	$\Delta B_v/B_v$ %	$D_v \times 10^7$ (cm^{-1})	$\Delta D_v/D_v$ %
$(1)^1\Pi$	0	267.12		0.2474 **0.2555**[a]	***3.2***	2.17 **2.28**[a]	***4.8***
	1	791.88		0.2448 **0.2539**[a]	***3.6***	2.29 **2.27**[a]	***0.9***
	2	1302.89		0.2431 **0.2523**[a]	***3.6***	1.83 **2.26**[a]	***19.0***
	3	1826.50		0.2424 **0.2507**[a]	***3.3***	1.92 **2.4**[a]	***20***
	4	2352.27		0.2408 **0.2493**[a]	***3.4***	2.16 **2.75**[a]	***21.5***
	5	2870.89		0.2395		2.07	
	6	3386.00		0.2383		1.98	
	7	3898.69		0.2368		1.97	
	8	4407.96		0.2352		1.80	
	9	4916.42		0.2338		2.15	
	10	5419.23		0.2326		1.99	
	11	5919.03		0.2313		2.09	
	12	6414.17		0.2299		1.72	
	13	6908.05		0.2284		1.99	
	14	7397.98		0.2272		1.97	
	15	7884.54		0.2259		1.99	
	16	8367.51		0.2247		1.92	
	17	8847.21		0.2233		1.79	
	18	9324.29		0.2220		1.92	
	19	9798.02		0.2207		1.94	

Continued

State	v	E_v (cm^{-1})	$\Delta E_v/E_v$ %	B_v (cm^{-1})	$\Delta B_v/B_v$ %	$D_v \times 10^7$ (cm^{-1})	$\Delta D_v/D_v$ %
	20	10,268.45		0.2195		1.94	
	21	10,735.52		0.2183		1.91	
	22	11,199.16		0.2169		2.01	
	23	11,658.60		0.2155		2.17	
	24	12,112.52		0.2138		2.36	
	25	12,559.51		0.2120		2.33	
State	v	E_v (cm^{-1})	$\Delta E_v/E_v$ %	B_v (cm^{-1})	$\Delta B_v/B_v$ %	$D_v \times 10^7$ (cm^{-1})	$\Delta D_v/D_v$ %
$X^1\Sigma_{0+}$	0	308.99		0.2678 **0.2669**[a]	***0.3***	2.03 **2.02**[a]	***0.5***
	1	922.72		0.2663 **0.2653**[a]	***0.4***	2.03 **2.03**[a]	***0.0***
	2	1531.26		0.2648 **0.2638**[a]	***0.4***	2.03 **2.07**[a]	***1.9***
	3	2134.66		0.2633 **0.2622**[a]	***0.4***	2.04 **2.03**[a]	***0.5***
	4	2733.03		0.2618 **0.2606**[a]	***0.5***	2.04 **2.15**[a]	***5.1***
	5	3326.41		0.2603		2.04	
	6	3914.88		0.2587		2.04	
	7	4498.49		0.2573		2.04	
	8	5077.31		0.2558		2.04	
	9	5651.39		0.2543		2.04	
	10	6220.78		0.2528		2.04	
	11	6785.55		0.2513		2.04	
	12	7345.73		0.2499		2.04	
	13	7901.35		0.2484		2.04	
	14	8452.41		0.2469		2.05	
	15	8998.87		0.2455		2.05	
	16	9540.74		0.2440		2.06	
State	v	E_v (cm^{-1})	$\Delta E_v/E_v$ %	B_v (cm^{-1})	$\Delta B_v/B_v$ %	$D_v \times 10^7$ (cm^{-1})	$\Delta D_v/D_v$ %
$(1)^3\Pi_{0+}$	0	289.92		0.2619 **0.2628**[a]	***0.3***	2.18 **2.07**[a]	***5.0***
	1	861.60		0.2603 **0.2611**[a]	***0.3***	2.19 **2.07**[a]	***5.5***
	2	1428.10		0.2587 **0.2596**[a]	***0.3***	2.19 **2.15**[a]	***1.8***
	3	1989.46		0.2571 **0.2579**[a]	***0.3***	2.19 **2.04**[a]	***6.8***
	4	2545.93		0.2555 **0.2563**[a]	***0.3***	2.20 **2.16**[a]	***1.8***
	5	3097.26		0.2539		2.19	
	6	3643.86		0.2523		2.20	
	7	4185.46		0.2508		2.20	
	8	4722.21		0.2492		2.19	
	9	5254.27		0.2476		2.22	
	10	5781.36		0.2460		2.19	
	11	6303.83		0.2445		2.20	
	12	6821.58		0.2429		2.22	
	13	7334.51		0.2414		2.19	
	14	7842.94		0.2398		2.21	
	15	8346.73		0.2383		2.22	
	16	8845.88		0.2367		2.19	

Table 3. Values of the eigenvalues, and the rotational constants for the different vibrational levels of the $(X)^1\Sigma^+$, $(1)^1\Pi$, $X^1\Sigma_{0+}$, and $(1)^3\Pi_{0+}$ states of LuF molecule comparison with the experimental values. Percentage relative error values are in [italics]. [a]Ref.[19], [b]Ref.[21], [c]Ref.[22]. Experimental values are indicated in bold.

State	v	E_v (cm^{-1})	B_v (cm^{-1})	$D_v \times 10^7$ (cm^{-1})
$(1)^1\Delta$	0	285.45	0.2470	1.91
	1	844.51	0.2451	2.07
	2	1384.91	0.2428	1.95
	3	1922.40	0.2421	1.44
	4	2478.01	0.2416	2.05
	5	3023.39	0.2396	2.10
	6	3560.15	0.2393	1.62
	7	4100.21	0.2376	2.06
	8	4631.67	0.2361	1.30
	9	5168.67	0.2348	2.24
	10	5695.63	0.2337	1.70
	11	6221.90	0.2327	2.17
	12	6740.65	0.2313	1.39
	13	7260.54	0.2299	1.95
	14	7775.19	0.2287	1.73
	15	8287.59	0.2276	2.07
	16	8794.49	0.2265	1.64
	17	9299.35	0.2250	1.75
	18	9800.97	0.2239	1.77
	19	10,299.37	0.2226	1.80
	20	10,794.44	0.2215	1.89
	21	11,285.70	0.2204	1.73
	22	11,774.06	0.2192	1.81
	23	12,259.04	0.2180	1.81
	24	12,740.76	0.2169	1.81
	25	13,219.23	0.2158	1.78
	26	13,694.62	0.2147	1.70
	27	14,167.30	0.2136	1.69
	28	14,637.38	0.2126	1.64
	29	15,105.25	0.2116	1.57
	30	15,571.48	0.2108	1.54
	31	16,036.29	0.2099	1.63
	32	16,498.82	0.2088	1.90
	33	16,957.05	0.2074	2.01
	34	17,410.40	0.2062	1.58
	35	17,861.88	0.2056	1.16
	36	18,314.20	0.2051	1.36
	37	18,766.02	0.2042	1.56
	38	19,216.01	0.2035	1.34
	39	19,665.26	0.2027	1.69
	40	20,111.24	0.2011	2.67
	41	20,548.26	0.1989	2.44
	42	20,977.96	0.1977	1.33
	43	21,406.64	0.1971	1.37
	44	21,834.37	0.1962	1.75
	45	22,258.90	0.1950	1.95
	46	22,679.15	0.1937	1.66
	47	23,096.78	0.1930	1.33
	48	23,513.27	0.1920	1.87
State	**v**	**E_v (cm^{-1})**	**B_v (cm^{-1})**	**$D_v \times 10^7$ (cm^{-1})**
$(2)^1\Sigma^+$	0	281.85	0.2481	1.97
	1	835.56	0.2459	2.04
	2	1377.97	0.2442	1.77
	3	1927.14	0.2433	1.82
	4	2476.49	0.2419	2.01

Continued

State	v	E_v (cm^{-1})	B_v (cm^{-1})	$D_v \times 10^7$ (cm^{-1})
	5	3018.93	0.2407	2.06
	6	3554.49	0.2395	1.85
	7	4087.64	0.2380	1.78
	8	4618.12	0.2361	1.71
	9	5147.01	0.2349	2.09
	10	5669.17	0.2336	2.01
	11	6186.57	0.2325	1.95
	12	6699.22	0.2308	1.61
	13	7210.38	0.2293	1.95
	14	7716.67	0.2281	1.94
	15	8218.83	0.2268	2.03
	16	8716.05	0.2255	1.78
	17	9210.01	0.2240	1.78
	18	9700.53	0.2227	1.90
	19	10,186.99	0.2214	1.93
	20	10,669.40	0.2201	1.91
	21	11,147.82	0.2188	1.85
	22	11,622.57	0.2175	1.87
	23	12,093.53	0.2162	1.91
	24	12,560.51	0.2149	1.94
	25	13,023.37	0.2136	1.92
	26	13,482.17	0.2122	1.84
	27	13,937.47	0.2110	1.72
	28	14,390.32	0.2100	1.62
	29	14,841.44	0.2090	1.68
	30	15,290.27	0.2079	1.87
	31	15,735.36	0.2065	1.99
	32	16,175.88	0.2051	1.95
	33	16,612.25	0.2039	1.73
	34	17,045.98	0.2030	1.54
	35	17,478.18	0.2020	1.80
	36	17,907.24	0.2007	1.95
	37	18,332.36	0.1996	1.54
	38	18,755.62	0.1986	1.88
	39	19,175.00	0.1970	2.37
	40	19,587.97	0.1954	1.94
	41	19,996.70	0.1941	1.95
	42	20,401.55	0.1929	1.63
	43	21,204.71	0.1908	2.16
	44	21,600.52	0.1895	1.69
	45	21,993.64	0.1885	1.64
	46	22,384.51	0.1875	1.72
State	v	E_v (cm^{-1})	B_v (cm^{-1})	$D_v \times 10^7$ (cm^{-1})
$(2)^1\Delta$	0	298.32	0.2500	1.88
	1	872.50	0.2483	1.90
	2	1438.61	0.2462	1.96
	3	1996.00	0.2451	1.62
	4	2561.73	0.2443	1.98
	5	3120.09	0.2431	2.05
	6	3669.88	0.2417	1.55
	7	4222.67	0.2402	1.86
	8	4770.06	0.2386	1.67
	9	5316.33	0.2375	2.15
	10	5854.51	0.2365	1.87
	11	6388.61	0.2349	1.54
Continued				

State	v	E_v (cm^{-1})	B_v (cm^{-1})	$D_v \times 10^7$ (cm^{-1})
	12	6921.84	0.2334	1.89
	13	7450.22	0.2323	1.84
	14	7974.84	0.2310	1.90
	15	8495.10	0.2299	1.88
	16	9011.11	0.2285	1.62
	17	9524.69	0.2270	1.81
	18	10,034.58	0.2259	2.00
	19	10,539.62	0.2248	1.72
	20	11,041.60	0.2234	1.75
	21	11,540.25	0.2222	1.84
	22	12,034.65	0.2210	1.72
	23	12,525.92	0.2197	1.75
	24	13,013.98	0.2187	1.83
State	v	E_v (cm^{-1})	B_v (cm^{-1})	$D_v \times 10^7$ (cm^{-1})
	0	278.67	0.2464	1.95
	1	832.20	0.2459	1.81
	2	1392.89	0.2445	1.91
	3	1948.86	0.2437	1.74
	4	2506.56	0.2420	1.92
	5	3057.91	0.2411	1.54
	6	3615.45	0.2406	1.90
	7	4167.59	0.2390	1.78
	8	4715.63	0.2374	2.04
	9	5255.11	0.2359	2.00
	10	5787.96	0.2347	1.59
	11	6320.48	0.2333	2.04
	12	6846.37	0.2321	1.75
	13	7369.55	0.2308	1.87
	14	7888.41	0.2295	1.83
	15	8403.70	0.2284	1.79
	16	8915.55	0.2270	1.79
	17	9424.25	0.2261	1.84
	18	9929.65	0.2249	1.57
	19	10,433.80	0.2239	1.71
$(1)^3\Delta$	20	10,935.74	0.2229	1.82
	21	11,434.08	0.2215	1.98
	22	11,926.72	0.2199	2.04
	23	12,413.50	0.2186	1.73
	24	12,897.79	0.2178	1.53
	25	13,380.72	0.2166	1.97
	26	13,858.62	0.2151	1.91
	27	14,332.35	0.2141	1.49
	28	14,804.72	0.2130	1.87
	29	15,272.95	0.2116	1.86
	30	15,737.47	0.2107	1.59
	31	16,199.93	0.2096	1.87
	32	16,658.46	0.2083	1.66
	33	17,114.55	0.2075	1.70
	34	17,568.14	0.2064	1.59
	35	18,019.76	0.2057	1.28
	36	18,471.35	0.2051	1.35
	37	18,922.85	0.2046	1.14
	38	19,375.16	0.2041	1.32
	39	19,826.94	0.2033	1.47
	40	20,277.26	0.2025	1.39

Continued

State	v	E_v (cm^{-1})	B_v (cm^{-1})	$D_v \times 10^7$ (cm^{-1})
	41	20,726.84	0.2021	0.85
	42	21,178.57	0.2022	0.62
	43	21,633.79	0.2021	1.14
	44	22,089.25	0.2012	1.78
	45	22,540.92	0.1999	1.63
	46	22,989.79	0.1994	0.70
State	**v**	**E_v (cm^{-1})**	**B_v (cm^{-1})**	**$D_v \times 10^7$ (cm^{-1})**
$(1)^3\Sigma^+$	0	278.57	0.2461	1.96
	1	829.37	0.2453	1.73
	2	1393.88	0.2442	1.90
	3	1952.13	0.2430	1.70
	4	2512.64	0.2417	1.87
	5	3067.08	0.2403	1.75
	6	3619.45	0.2391	2.06
	7	4162.04	0.2374	1.77
	8	4701.22	0.2359	1.80
	9	5237.53	0.2351	1.67
	10	5773.28	0.2339	1.88
	11	6303.65	0.2322	1.80
	12	6830.34	0.2313	1.76
	13	7354.17	0.2299	1.79
	14	7874.21	0.2287	1.84
	15	8390.21	0.2275	1.70
	16	8903.40	0.2262	1.79
	17	9412.90	0.2251	1.83
	18	9918.65	0.2239	1.68
	19	10,421.56	0.2226	1.77
	20	10,921.00	0.2214	1.82
	21	11,416.65	0.2202	1.79
	22	11,908.43	0.2189	1.72
	23	12,396.92	0.2178	1.80
	24	12,881.87	0.2166	1.71
	25	13,363.76	0.2154	1.77
	26	13,842.04	0.2142	1.76
	27	14,317.02	0.2131	1.75
	28	14,788.75	0.2119	1.71
	29	15,257.25	0.2107	1.75
	30	15,722.51	0.2097	1.75
	31	16,184.57	0.2085	1.69
	32	16,643.55	0.2074	1.66
	33	17,099.78	0.2064	1.65
	34	17,553.40	0.2054	1.49
	35	18,005.30	0.2046	1.34
	36	18,456.59	0.2039	1.26
	37	18,907.89	0.2034	1.15
State	**v**	**E_v (cm^{-1})**	**B_v (cm^{-1})**	**$D_v \times 10^7$ (cm^{-1})**
$(2)^3\Delta$	0	268.31	0.2437	1.93
	1	815.15	0.2432	1.78
	2	1369.84	0.2416	1.85
	3	1921.58	0.2410	1.82
	4	2471.31	0.2397	1.42
	5	3031.93	0.2395	1.57
	6	3595.88	0.2385	1.96
	7	4150.01	0.2367	2.09

Continued

State	v	E_v (cm^{-1})	B_v (cm^{-1})	$D_v \times 10^7$ (cm^{-1})
	8	4691.83	0.2348	1.81
	9	5228.57	0.2336	1.81
	10	5761.25	0.2322	1.91
	11	6288.51	0.2310	1.78
	12	6811.99	0.2296	1.74
	13	7332.04	0.2283	1.90
	14	7847.43	0.2272	1.82
	15	8358.92	0.2258	1.66
	16	8867.80	0.2247	1.82
	17	9373.18	0.2237	1.71
	18	9876.10	0.2226	1.55
	19	10,377.73	0.2216	1.78
	20	10,875.92	0.2203	1.93
	21	11,368.69	0.2187	2.03
	22	11,855.10	0.2173	1.78
	23	12,338.18	0.2164	1.54
	24	12,819.98	0.2153	1.84
	25	13,297.47	0.2138	1.97
	26	13,770.00	0.2128	1.54
	27	14,240.95	0.2118	1.77
	28	14,708.29	0.2104	1.86
	29	15,171.56	0.2094	1.54
	30	15,633.00	0.2084	1.80
State	v	E_v (cm^{-1})	B_v (cm^{-1})	$D_v \times 10^7$ (cm^{-1})
$(1)^3\Pi$	0	291.50	0.2536	2.00
	1	860.03	0.2518	1.83
	2	1437.25	0.2511	1.81
	3	2016.09	0.2494	1.83
	4	2592.79	0.2486	1.78
	5	3168.65	0.2471	1.87
	6	3739.56	0.2459	1.66
	7	4311.43	0.2449	1.83
	8	4878.95	0.2433	2.12
	9	5435.77	0.2415	1.98
	10	5985.38	0.2399	1.64
	11	6535.18	0.2395	1.60
	12	7084.97	0.2379	2.12
	13	7626.12	0.2364	1.72
	14	8165.00	0.2355	1.75
	15	8701.13	0.2340	1.96
	16	9231.76	0.2328	1.70
	17	9759.94	0.2316	1.89
	18	10,283.71	0.2303	1.71
	19	10,804.50	0.2290	1.80
	20	11,321.75	0.2279	1.67
	21	11,836.59	0.2268	1.78
	22	12,348.23	0.2257	1.75
	23	12,856.65	0.2244	2.00
	24	13,359.71	0.2230	1.89
	25	13,858.25	0.2217	1.77
	26	14,353.59	0.2207	1.63
	27	14,846.60	0.2195	1.90
	28	15,335.15	0.2181	1.78
	29	15,820.08	0.2170	1.69
	30	16,302.28	0.2159	1.81

Continued

State	v	E_v (cm^{-1})	B_v (cm^{-1})	$D_v \times 10^7$ (cm^{-1})
	31	16,780.84	0.2146	1.83
	32	17,255.66	0.2135	1.68
	33	17,727.74	0.2124	1.84
	34	18,196.14	0.2112	1.73
	35	18,661.43	0.2101	1.67
	36	19,124.05	0.2090	1.69
	37	19,584.04	0.2081	1.45
	38	20,042.81	0.2074	1.38
	39	20,500.93	0.2068	1.22
	40	20,959.33	0.2063	1.23

Table 4. Values of the eigenvalues, and the rotational constants for the different vibrational levels of the low-lying states $(1)^1\Delta$, $(2)^1\Sigma^+$, $(2)^1\Delta$, $(1)^3\Delta$, $(1)^3\Sigma^+$, $(2)^3\Delta$, and $(1)^3\Pi$ of LuF molecule.

$(1)^3\Pi_{0+} \longrightarrow X^1\Sigma_{0+}$						
$\left(v'' = 0 - v = 0\right)$ Band						
J	P–branch	Shift value (in cm^{-1}) $\widetilde{\nu}[P(J)]_{exp} - \widetilde{\nu}[P(J)]_{theo}$	Error (%)	R–branch	Shift value (in cm^{-1}) $\widetilde{\nu}[R(J)]_{exp} - \widetilde{\nu}[R(J)]_{theo}$	Error (%)
0						
1						
2				14,992.29 **16,154.31**[a]	1162.02	*7.2*
3				14,992.78 **16,154.8**[a]	1162.02	*7.2*
4	14,988.54 **16,150.56**[a]	1162.02	*7.2*	14,993.26 **16,155.29**[a]	1162.03	*7.2*
5	14,987.96 **16,149.97**[a]	1162.01	*7.2*	14,993.72 **16,155.74**[a]	1162.02	*7.2*
6	14,987.36 **16,149.41**[a]	1162.05	*7.2*	14,994.17 **16,156.24**[a]	1162.07	*7.2*
7	14,986.76 **16,148.82**[a]	1162.06	*7.2*	14,994.61 **16,156.7**[a]	1162.09	*7.2*
8	14,986.14 **16,148.23**[a]	1162.09	*7.2*	14,995.04 **16,157.16**[a]	1162.12	*7.2*
9	14,985.51 **16,147.63**[a]	1162.12	*7.2*	14,995.46 **16,157.62**[a]	1162.16	*7.2*
10	14,984.87 **16,147.02**[a]	1162.15	*7.2*	14,995.87 **16,158.06**[a]	1162.19	*7.2*
11	14,984.22 **16,146.4**[a]	1162.18	*7.2*	14,996.26 **16,158.49**[a]	1162.23	*7.2*
12	14,983.55 **16,145.78**[a]	1162.23	*7.2*	14,996.64 **16,158.91**[a]	1162.27	*7.2*
13	14,982.87 **16,145.16**[a]	1162.29	*7.2*	14,997.01 **16,159.34**[a]	1162.33	*7.2*
14	14,982.18 **16,144.51**[a]	1162.33	*7.2*	14,997.37 **16,159.74**[a]	1162.37	*7.2*
15	14,981.48 **16,143.85**[a]	1162.37	*7.2*	14,997.72 **16,160.15**[a]	1162.43	*7.2*
16	14,980.77 **16,143.18**[a]	1162.41	*7.2*	14,998.05 **16,160.53**[a]	1162.48	*7.2*
17	14,980.05 **16,142.56**[a]	1162.51	*7.2*	14,998.37 **16,160.93**[a]	1162.56	*7.2*
18	14,979.31 **16,141.86**[a]	1162.55	*7.2*	14,998.68 **16,161.3**[a]	1162.62	*7.2*
19	14,978.56 **16,141.18**[a]	1162.62	*7.2*	14,998.98 **16,161.66**[a]	1162.68	*7.2*
20	14,977.81 **16,140.56**[a]	1162.75	*7.2*	14,999.27 **16,162.03**[a]	1162.76	*7.2*

Table 5. The theoretical wavenumbers (in cm^{-1}) of the rotation lines of the electronic spectrum of LuF molecule compared with the available experimental values. Percentage relative error values are in [italics]. [a]Ref.[19]. Experimental values are indicated in bold.

$$\tilde{\nu} = \tilde{\nu}_0 + (B_{v'} + B_{v''})m + (B_{v'} - B_{v''} - D_{v'} + D_{v''})m^2 - 2(D_{v'} + D_{v''})m^3 + (D_{v''} - D_{v'})m^4 \quad (1)$$

where $\tilde{\nu}_0$ is the vibrational transition band center, $B_{v'}$ and $B_{v''}$ are the rotational constants for the $(1)^3\Pi_{0+}$ (upper vibrational state) and $X^1\Sigma_{0+}$ (lower vibrational state) respectively, $D_{v'}$ is the centrifugal distortion constant for the upper vibrational state, and $D_{v''}$ is the centrifugal distortion constant for the lower vibrational state. Comparing these values with those reported by Effantin et al.[19] yields a good agreement, where the percentage relative difference is 7.2% for the P and R branches. At the same time, the constant shift ($\sim 1162\text{cm}^{-1}$), which corresponds to a relative difference of approximately 7.2% among all presented ro-vibrational energy levels shows that there may have been an experimental setting in[19] (possible calibration issues) that would have led to a discrepancy in the vibrational transition band center value $\tilde{\nu}_0$, that propagated to all investigated rotational levels.

The fine structure selection rules state that the transitions $\Sigma-\Delta$, $\Delta\Omega > 1$, and 0^+-0^- are forbidden[20]. Consequently, we analyzed only the transitions $^1\Pi - {}^1\Sigma^+$, $^1\Pi - {}^1\Delta$ among the lowest states shown in Fig. 3. More precisely, we present their Transition Dipole Moment (TDM) curves in the considered region $1.5\ \text{Å} \leq R \leq 2.12\ \text{Å}$ in Fig. 4. We then deduced the electronic emission coefficients proposed by Hilborn et al.[37], based on the values of the transitions' dipole moments at the equilibrium positions of the upper states for each electronic transition $|\mu_{21}|$:

$$\omega_{ij} = 2\pi\nu_{ij} \quad (2)$$

$$A_{ij} = \frac{2\omega_{ij}^3\mu_{ij}^2}{3\varepsilon_0 hc^3} \quad (3)$$

$$\gamma_{cl} = \frac{e^2\omega_{ij}^2}{6\pi\varepsilon_0 m_e c^3} \quad (4)$$

$$f_{ij} = \frac{-A_{ij}}{3\gamma_{cl}} \quad (5)$$

ω_{21} is the emission angular frequency and A_{21} is the Einstein coefficients for spontaneous emissions. For the perpendicular transitions with $\Delta\Lambda = \pm 1$ (or $\Delta\Omega = \pm 1$) such as $^1\Pi - {}^1\Sigma^+$, $^1\Pi - {}^1\Delta$, the Einstein coefficient A_{ij} must be divided by an additional factor of two[38] depending on the exact definition of μ_{ij}. The constants ε_0 and m_e are respectively the vacuum permittivity and the mass of the electron. $|f_{21}|$, γ_{cl}, and ν_{ij} are respectively the oscillator strength constant, the classical radiative decay rate of the single-electron oscillator, and the transition frequency between the two states. h and c represent the Planck constant and the speed of light, respectively. The calculated values of these constants for the two transitions $(1)^3\Pi_{0+} - X^3\Sigma_{0+}$ and $(1)^3\Pi_{0+} - (1)^3\Delta_1$ are given in Table 6. No comparison of these results with literature is available since they are given here for the first time. However, the value of the radiative lifetime τ will be discussed in the next section.

Laser cooling study of LuF molecule

The difference in the values of the equilibrium positions ΔR_e between the ground $X^1\Sigma_{0+}$ and $(1)^3\Pi_{0+}$ and $(1)^3\Delta_1$ states of LuF molecule is minimal, which is an encouraging factor in verifying the laser cooling feasibility for this molecule. The main criteria to keep a closed-loop cycle in a laser cooling process are:

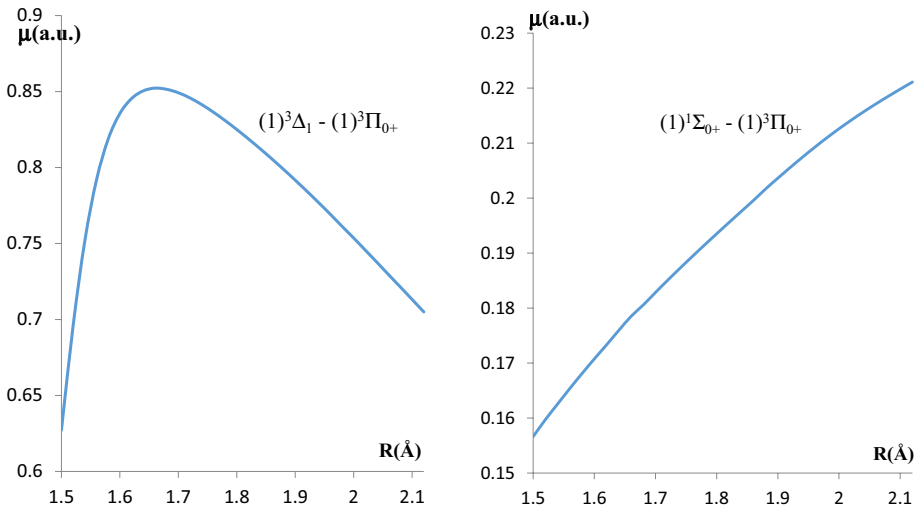

Figure 4. The transition dipole moment curves for the $X^1\Sigma_{0+}-(1)^3\Pi_{0+}$ and $(1)^3\Delta_1 - (1)^3\Pi_{0+}$ transitions of LuF molecule.

LuF-SO						
Transition	**$\|\mu_{21}\|$(a.u.)**	**$\omega_{21} \times 10^{-15}$ (rads^{-1})**	**A_{21} (s^{-1})**	**τ_{21}(s)**	**$\gamma_{cl} \times 10^{-6}$(s^{-1})**	**$\|f_{21}\|$**
$X^1\Sigma_{0+}-(1)^3\Pi_{0+}$	0.2126	2.826	3.1×10^5	3.235×10^{-6}	50.0	0.00206
$(1)^3\Delta_1-(1)^3\Pi_{0+}$	0.7536	0.2807	3.8×10^3	2.625×10^{-4}	0.494	0.00258

Table 6. The transition dipole moment values at the upper state equilibrium position $|\mu_{21}|$, the emission angular frequency ω_{21}, the Einstein spontaneous coefficients A_{21}, the spontaneous radiative lifetime τ_{21}, the classical radiative decay rate of the single-electron oscillator γ_{cl}, and the emission oscillator strength f_{21} of some transitions among the doublet states of LuF molecule.

1. A highly diagonal Franck–Condon factor (FCF) among the lowest vibrational levels of the ground and considered excited states.
2. The absence of an intervening intermediate state, unless it was found possible to include it within the laser cooling scheme.
3. A short radiative lifetime of a given transition (in the range of ns to μs) ensures a rapid spontaneous deexcitation of the molecules to provide a high number of cycles per second.

We consequently calculated the FCF values among specific states using LEVEL 11 program[39]. Our results for the allowed transitions $(1)^3\Pi_{0+} - X^3\Sigma_{0+}$ and $(1)^3\Pi_{0+} - (1)^3\Delta_1$ show a diagonal FCF among the first three vibrational levels for the two transitions, as shown in Fig. 5.

To probe how substantially an intermediate state influences a given cooling cycle, one can rely upon the vibrational branching ratio loss $\left(\gamma = \left(A_{v''v'-\text{Excited/Intermediate}}\right)/\left(A_{v''v-\text{Excited/Ground}}\right)\right)$ between the considered intermediate state and the excited state involved in the cooling process. Here, $A_{v''v'-\text{Excited/Intermediate)}}$ is the Einstein coefficient for transitions between the excited and Intermediate states, and $A_{v''v-\text{excited/ground}}$ is that for transitions between the excited and ground-state. If the value of γ is less than 10^{-4}, then the intermediate state should have a minimal effect on the cooling cycle[40].

In our case, we follow a similar procedure to understand the implication of the intermediate state $(1)^3\Delta_1$, in a cooling loop cycle consisting of the ground state $X^1\Sigma_{0+}$, and the excited state $(1)^3\Pi_{0+}$. In general, Einstein's coefficient $A_{v'v}$ among vibrational levels can be written as the following[41]:

$$A_{v'v} = ((3.1361891)\left(10^{-7}\right)(\Delta E)^3\left(\psi_{v'}|M(r)|\psi_v\right)^2) \tag{6}$$

where ΔE is the emission frequency (in cm^{-1}), and M(r) is the electronic transition dipole moment between the two electronic states that are considered (in Debye).

Our calculated value of the transition dipole moment, obtained with the Molpro software[30], is vertical (given as μ_x, μ_y, and μ_z)). In our calculations, we choose the highest value of these transition matrix elements (μ_x in this case). Consequently, we considered the Einstein coefficient $A_{v'v}$ (Eq. (2)) to be:

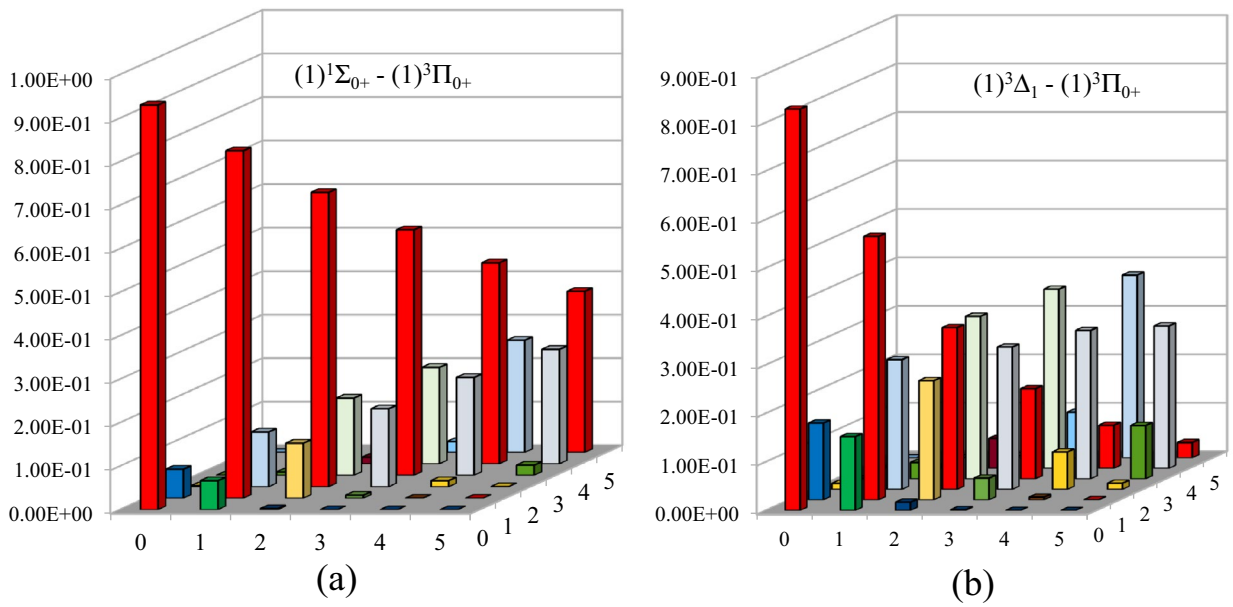

Figure 5. The Franck-Condon factor for $X^1\Sigma_{0+} - (1)^3\Pi_{0+}$ and $(1)^3\Delta_1 - (1)^3\Pi_{0+}$ transitions of LuF molecule.

$$A_{\nu'\nu} = ((3.1361891)(10^{-7})(\Delta E)^3(\psi_{\nu'}|\mu_x|\psi_\nu)^2) \quad (7)$$

The values of the vibrational branching ratio for the first five vibrational levels, which represents the percentage of transition probability between two vibrational levels, are given in Tables 7, 8 and are obtained by using the formula[42]:

$$R_{\nu'\nu} = \frac{A_{\nu'\nu}}{\sum_\nu A_{\nu'\nu}} \quad (8)$$

Finally, each transition's radiative lifetimes are calculated using $\tau(s) = 1/\sum_\nu A_{\nu'\nu,}$ and presented in Table 7 and Table 8. Up to our knowledge, the radiative lifetimes of LuF molecule spin–orbit states are presented here for the first time in the literature. One can notice that the spontaneous emission of the transition $(1)^3\Pi_{0+} - X^3\Sigma_{0+}$ is dominant over that of $(1)^3\Pi_{0+} - (1)^3\Delta_1$, where the FCF and the radiative lifetime of the former are $f_{00} = 0.930636$ and $\tau = 3.45$ µs while those of the later are $f_{00} = 0.828539$ and $\tau = 0.259$ ms. The variation in the radiative lifetime for the two transitions is due to the difference in energy ΔE, which is much more important between the ground state $X^1\Sigma_{0+}$ and the excited state $(1)^3\Pi_{0+}$, compared to that between the excited state $(1)^3\Pi_{0+}$ and the intermediate state $(1)^3\Delta_1$. The comparison of these values for the radiative lifetime with those calculated by using Hilborn emission coefficients[37] that are given in Table 6 for the two transitions $(1)^3\Pi_{0+} - X^3\Sigma_{0+}$ and $(1)^3\Pi_{0+} - (1)^3\Delta_1$ shows an excellent agreement with the relative differences 6.2% and 1.3% respectively.

Our calculated value for the vibrational branching loss ratio $\gamma = \gamma_\Delta/\gamma_\Sigma = 0.02812$ where, γ_Δ and γ_Σ represent the total emission rate of the $(1)^3\Pi_{0+} - (1)^3\Delta_1$, and $(1)^3\Pi_{0+} - X^1\Sigma_{0+}$ transitions, respectively. The order of this ratio is two times higher than the minimum required value of 10^{-4}[40]. Consequently, the intermediate state $(1)^3\Delta_1$ must be considered while setting a convenient laser cooling scheme. At the same time, the forbidden transitions $(1)^3\Pi_{0+} - (1)^3\Pi_{0-}$, $(1)^3\Pi_{0+} - (1)^3\Delta_2$, and $X^1\Sigma_{0+} - (1)^3\Delta_2$[20] do not disturb the transition $X^1\Sigma_{0+} - (1)^3\Pi_{0+}$.

Laser cooling schemes with an intermediate state have already been proposed in the literature[43,44]. We use the technique proposed by Yuan et al.[41] to include the intermediate state in the laser cooling cycle. To this end, one must calculate the Einstein coefficients for transitions among the three involved electronic states, i.e., $X^1\Sigma_{0+}$, $(1)^3\Pi_{0,}$ and $(1)^3\Delta_{1.}$ For the two transitions $(1)^3\Pi_{0+} - X^3\Sigma_{0+}$ and $(1)^3\Pi_{0+} - (1)^3\Delta_1$, the values of the vibrational branching ratio for the first five vibrational levels are given in Table 9 by using the formulas:

$$(1)^3\Pi_{0+} - X^1\Sigma_{0+} \rightarrow R_{\nu''\nu} = \frac{A_{\nu''\nu}}{\sum_\nu A_{\nu''\nu} + \sum_{\nu'} A_{\nu''\nu'}} \quad (9)$$

$$(1)^3\Pi_{0+} - (1)^3\Sigma_1 \rightarrow R'_{\nu''\nu'} = \frac{A_{\nu''\nu'}}{\sum_\nu A_{\nu''\nu} + \sum_{\nu'} A_{\nu''\nu'}} \quad (10)$$

$A_{\nu''\nu}$ and $A_{\nu''\nu'}$ are the Einstein coefficients for the transitions $(1)^3\Pi_{0+}$–$X^1\Sigma_{0+}$ and $(1)^3\Pi_{0+}$–$(1)^3\Delta_1$, respectively. For the main optical cycle of the transition $(1)^3\Pi_{0+} - X^1\Sigma_{0+}$, the number of cycles (N) for photon absorption/emission among vibrational levels (denoted as a, b, c, etc.…) is reciprocal to the total loss:

LuF-SO								
	$\nu_{''}((1)^3\Pi_{0+}) = 0$		1	2	3	4	5	6
$\nu\,(X^1\Sigma_{0+}) = 0$	$A_{\nu''\nu}$	269,977.6372	18,918.19075	642.7389436	10.37449812	0.008082286	0.007478636	1.08E−04
	$R_{\nu''\nu}$	0.93012820	0.06540194	0.00224561	0.00003631	0.00000003	0.00000003	0.00000000
$\nu = 1$	$A_{\nu''\nu}$	19,607.00055	231,378.8478	35,777.64278	1968.533459	47.14847216	0.155388532	0.027200272
	$R_{\nu''\nu}$	0.06755013	0.79989809	0.12500066	0.00689015	0.00016637	0.00000057	0.00000016
$\nu = 2$	$A_{\nu''\nu}$	662.5329264	36,962.71764	193,724.8751	50,607.33398	3957.673996	133.1030565	0.860364798
	$R_{\nu''\nu}$	0.00228256	0.12778354	0.67683995	0.17713293	0.01396533	0.00049230	0.00000496
$\nu = 3$	$A_{\nu''\nu}$	11.23597355	1953.886076	52,100.03828	161,755.6346	63,227.53364	6604.88765	293.2955742
	$R_{\nu''\nu}$	0.00003871	0.00675476	0.18202819	0.56616793	0.22310912	0.02442886	0.00169205
$\nu = 4$	$A_{\nu''\nu}$	0.114685072	46.11648268	3853.65538	64,779.67216	131,027.7702	73,541.16762	9890.39006
	$R_{\nu''\nu}$	0.00000040	0.00015943	0.01346398	0.22673815	0.46235381	0.27199960	0.05705855
$\nu = 5$	$A_{\nu''\nu}$	0.000877974	0.642376596	118.627261	6336.161712	75,768.21386	105,399.3421	81,877.02166
	$R_{\nu''\nu}$	0.00000000	0.00000222	0.00041446	0.02217747	0.26736105	0.38983035	0.47235587
$\nu = 6$	$A_{\nu''\nu}$	7.34E−05	0.007381814	2.04282127	244.8646484	9364.514784	84,693.67356	81,275.97982
	$R_{\nu''\nu}$	0.00000000	0.00000003	0.00000714	0.00085706	0.03304429	0.31324830	0.46888841
Sum $(s^{-1}) = A_{\nu''\nu}$		290,258.5223	289,260.4085	286,219.6205	285,702.5751	283,392.8630	270,372.3369	173,337.5748
$\tau:(s) = 1/A_{\nu''\nu}$		3.4452E−06	3.45709E−06	3.49382E−06	3.50014E−06	3.52867E−06	3.6986E−06	5.76909E−06
τ:(µs)		3.45	3.46	3.49	3.50	3.53	3.70	5.77

Table 7. The radiative lifetimes τ, and the vibrational branching ratio of the vibrational transitions between the electronic states $(1)^3\Pi_{0+}$–$X^1\Sigma_{0+}$ of the molecule LuF.

LuF-SO								
	$v''((1)^3\Pi_{0+})=0$		1	2	3	4	5	6
$v'((1)^3\Delta_1)=0$	$A_{v''v'}$	3795.717704	420.4072658	420.4072658	0.014461864	7.04748E−05	0.000178738	9.99366E−05
	$R_{v''v'}$	0.98478369	0.05448771	0.05448771	0.00000185	0.00000001	0.00000002	0.00000001
$v'=1$	$A_{v''v'}$	58.52845986	7182.184544	7182.184544	0.155152468	0.071005714	0.00084819	0.00012794
	$R_{v''v'}$	0.01518497	0.93086119	0.93086119	0.00001986	0.00000904	0.00000011	0.00000002
$v'=2$	$A_{v''v'}$	0.12764095	112.6588205	112.6588205	1185.079902	0.233541534	0.185820348	0.004076242
	$R_{v''v'}$	0.00003312	0.01460137	0.01460137	0.15171184	0.00002974	0.00002355	0.00000054
$v'=3$	$A_{v''v'}$	−0.00141388	0.410281126	0.410281126	6413.38877	1538.539034	0.291628088	0.393386436
	$R_{v''v'}$	−0.00000037	0.00005318	0.00005318	0.82103072	0.19594947	0.00003696	0.00005190
$v'=4$	$A_{v''v'}$	−0.003770594	−0.004047702	−0.004047702	211.2423738	6056.0312	1872.106295	0.309794184
	$R_{v''v'}$	−0.00000098	−0.00000052	−0.00000052	0.02704288	0.77130060	0.23729473	0.00004087
$v'=5$	$A_{v''v'}$	−0.00134734	−0.016112822	−0.016112822	1.516054618	254.470936	5722.200736	2167.619392
	$R_{v''v'}$	−0.00000035	−0.00000209	−0.00000209	0.00019408	0.03240961	0.72530501	0.28597214
$v'=6$	$A_{v''v'}$	−0.000308208	−0.006421308	−0.006421308	−0.009631366	2.367540836	294.5860572	5411.500234
	$R_{v''v'}$	−0.00000008	−0.00000083	−0.00000083	−0.00000123	0.00030153	0.03733961	0.71393452
Sum $(s^{-1})=A_{v''v'}$		3854.366965	7715.63433	7715.63433	7811.387084	7851.713329	7889.371564	7579.827111
τ: (s) $=1/A_{v''v'}$		0.000259446	0.000129607	0.000129607	0.000128018	0.000127361	0.000126753	0.000131929
τ: (ms)		0.259	0.130	0.130	0.128	0.127	0.127	0.132

Table 8. The radiative lifetimes τ, and the vibrational branching ratio of the vibrational transitions between the electronic states $(1)^3\Pi_{0+}$–$(1)^3\Delta_1$ of the molecule LuF.

	$v''((1)^3\Pi_{0+})=0$		1	2	3	4	5
$v\,(X^1\Sigma_{0+})=0$	$A_{v''v}$	269,977.6372	18,918.19075	642.7389436	10.37449812	0.008082286	0.007478636
	$R_{v''v}$	0.917938781	0.063702883	0.002187566	0.002187566	3.9262E−08	9.10342E−08
$v=1$	$A_{v''v}$	19,607.00055	231,378.8478	35,777.64278	1968.533459	47.14847216	0.155388532
	$R_{v''v}$	0.066664878	0.77911783	0.121769445	0.006860641	0.000229037	1.89148E−06
$v=2$	$A_{v''v}$	662.5329264	36,962.71764	193,724.8751	50,607.33398	3957.673996	133.1030565
	$R_{v''v}$	0.002252648	0.124463894	0.659343902	0.176374314	0.019225541	0.001620207
$v=3$	$A_{v''v}$	11.23597355	1953.886076	52,100.03828	161,755.6346	63,227.53364	6604.88765
	$R_{v''v}$	3.82029E−05	0.006579285	0.177322827	0.563743174	0.307145956	0.080398471
$v=4$	$A_{v''v}$	0.114685072	46.11648268	3853.65538	64,779.67216	131,027.7702	73,541.16762
	$R_{v''v}$	3.89936E−07	0.000155287	0.013115942	0.225767084	0.636505134	0.895185167
$v'((1)^3\Delta_1)=0$	$A_{v''v'}$	3795.717704	420.4072658	420.4072658	0.014461864	7.04748E−05	0.000178738
	$R'_{v''v'}$	0.012905648	0.00141563	0.001430859	5.04018E−08	3.42352E−10	2.17571E−09
$v'=1$	$A_{v''v'}$	58.52845986	7182.184544	7182.184544	0.155152468	0.071005714	0.00084819
	$R'_{v''v'}$	0.000199	0.024184441	0.024444613	5.4073E−07	3.44931E−07	1.03246E−08
$v'=2$	$A_{v''v'}$	0.12764095	112.6588205	112.6588205	1185.079902	0.233541534	0.185820348
	$R'_{v''v'}$	4.33986E−07	0.000379354	0.000383435	0.004130185	1.1345E−06	2.26191E−06
$v'=3$	$A_{v''v'}$	0.00141388	0.410281126	0.410281126	6413.38877	1538.539034	0.291628088
	$R'_{v''v'}$	4.80727E−09	1.38153E−06	1.39639E−06	0.022351643	0.007473897	3.54986E−06
$v'=4$	$A_{v''v'}$	0.003770594	0.004047702	0.004047702	211.2423738	6056.0312	1872.106295
	$R'_{v''v'}$	1.28202E−08	1.36298E−08	1.37764E−08	0.000736212	0.029418916	0.022788349
$\sum_{v} A_{v''v} + \sum_{v'} A_{v''v'}$		294,112.9003	296,975.4237	293,814.6154	286,931.4294	205,855.0092	82,151.90596
$\tau=1/(\sum_{v} A_{v''v} + \sum_{v'} A_{v''v'}$		3.40005E−06	3.36728E−06	3.40351E−06	3.48515E−06	4.85779E−06	1.21726E−05
τ (μs)		3.40	3.37	3.40	3.49	4.86	12.17

Table 9. The radiative lifetimes τ, and the vibrational branching ratio of the vibrational transitions between the electronic states $(1)^3\Pi_{0+}$–$X^1\Sigma_{0+}$ and $(1)^3\Pi_{0+}$–$(1)^3\Delta_1$ of the molecule LuF.

$$N = \frac{1}{1 - \left[(R_{00} + R'_{00} + R_{0a} + R'_{0a} \ldots) + (R_{0b} + R'_{0b} + R_{0c} + R'_{0c} \ldots.)\left(R_{a0} + R'_{a0} + R_{aa} + R'_{ab} + \ldots.\right)\right]} \tag{11}$$

Having the value of N, the experimental parameters needed to realize the cooling of a molecule can be obtained. If k_b and h are the Boltzmann and Planck constants, and m is the mass of the molecule, the mathematical expressions of these parameters are[45]:

$$V = \frac{hN}{m\lambda_{00}} \tag{12}$$

$$\mathrm{T_{ini}} = \frac{mV^2}{2k_B} \tag{13}$$

$$\mathrm{a_{max}} = \frac{hN_e}{N_{tot}m\lambda_{00}\tau} \tag{14}$$

$$L = \frac{k_B T_{ini}}{ma_{max}} \tag{15}$$

where V and $\mathrm{T_{ini}}$ are the initial velocity and temperature of the molecule, respectively. The maximum acceleration is $\mathrm{a_{max}}$, and the slowing distance is L. $\mathrm{N_e}$ is the number of excited states in the main cycling transition and $\mathrm{N_{tot}}$ is the number of the excited states connected to the ground state plus $\mathrm{N_e}$.

We considered the cooling scheme presented in Fig. 6 to obtain suitable experimental values. The driving lasers are given in solid lines for the two transitions along with their corresponding wavelengths. Dotted lines represent the spontaneous decays with the values of their FCF ($\mathrm{f_{v''v}}$ and $\mathrm{f'_{v''v'}}$) and the vibrational branching ratios $R_{v''v}$ and $R'_{v''v'}$. The suggested scheme includes the two transitions $X^1\Sigma_{0+} - (1)^3\Pi_{0+}$ and $(1)^3\Pi_{0+} - (1)^3\Delta_1$. The wavelength of the main cycling laser for the transition $X^1\Sigma_{0+} - (1)^3\Pi_{0+}$ is $\lambda_{00} = 336.8$ nm, while that of the repump laser is $\lambda_{01} = 343.8$ nm. Since the influence of the intermediate state $(1)^3\Delta_1$ cannot be ignored, there is

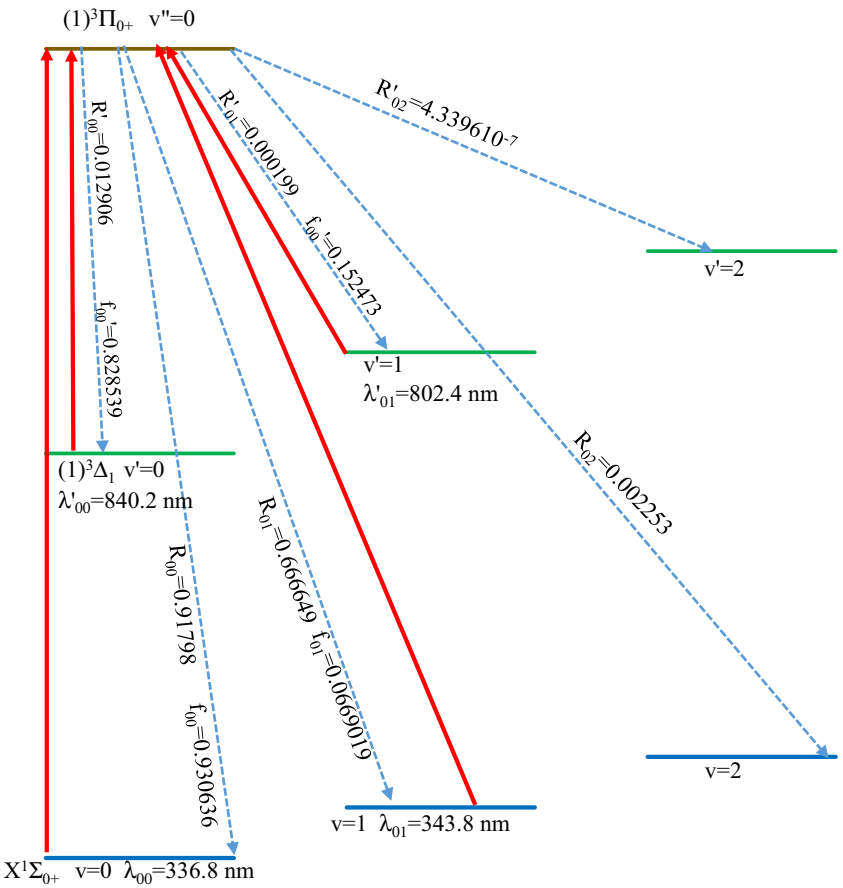

Figure 6. The laser cooling scheme of $X^1\Sigma_{0+} - (1)^3\Pi_{0+}$ and $(1)^3\Delta_1 - (1)^3\Pi_{0+}$ transitions of LuF molecule.

a need for two additional lasers to handle the loss to the vibrational levels for the transition $(1)^3\Pi_{0+} - (1)^3\Delta_1$, at $\lambda'_{00} = 840.2$ nm and $\lambda'_{01} = 802.4$ nm.

The value of N for this scheme is calculated as the following:

$$N = \frac{1}{1 - [(R_{00} + R'_{00} + R_{01} + R'_{01})} \tag{16}$$

The corresponding experimental parameters for this scheme are N = 442, L = 1.04 cm,V = 2.73 m/s, $T_{ini} = 86.7$ mK, $a_{max} = 358$ m/s^2, and $N_e/N_{tot} = 1/3$. The temperatures that can be reached during the cooling process can be obtained by calculating the Doppler limit temperature T_D and the recoil temperature T_r[42]:

$T_D = \frac{h}{4k_B\pi\tau} = 1108.6nK$ and $T_r = \frac{h^2}{mk_B\lambda_{00}^2} = 888mK$

Suppose T_i is the temperature of the LuF molecules obtained by using laser ablation to produce the atoms of the LuF molecule[46], typically in the order of $T_i = 7000$ K. In that case, there is a need for an intermediate process for the molecules to reach the mK regime. This regime can be obtained by collisions between LuF hot molecules of mass M, and cold buffer helium gas of mass m and temperature T_B. After N collision, the temperature T_N of the molecule is given by[47]:

$$T_N = T_B + (T_i - T_B)\exp\left(-2Mm/(M + m)^2\right)N \tag{17}$$

We suggest a pre-cooling temperature for LuF molecule $T_N = 86.7$ mK, corresponding to T_{ini} of the laser cooling process, and a helium gas temperature $T_B = 2$ K. From Eq. (6), the number of collisions in the buffer cell equals N = 285. At low temperatures in the buffer gas cell, the collision between the molecules can be ignored. If the density of helium $n_{He} = 5 \times 10^{14}$ cm^3 and the collision cross-section $\sigma_{X-He} = 10^{-14}$ cm^2 the average distance (mean free path) λ between two collisions is given by[48]

$$\lambda = 1/\left((\sigma_{X-He} \cdot n_{He})(1 + M/m)^{1/2}\right) \tag{18}$$

The corresponding value of λ = 0.0287 cm. Based on the rules of the kinetic theory of ideal gases, the molecules in the buffer gas cell will be thermalized during the time[48]:

$$t = \sum_{N=0}^{98} \frac{\lambda}{\sqrt{\frac{3k_b}{M}(T_i - T_B)e^{-N/\kappa} + T_i}} \tag{19}$$

where $\kappa = \frac{(M+m)^2}{2mM}$. During this short time, t = 0.444 ms in the buffer gas, the LuF molecules will reach a suitable before being sent to the Doppler laser cooling setup.

Conclusion

The adiabatic potential energy curves for the singlet and triplet electronic states of the LuF molecule have been investigated with spin–orbit calculation upon employing the MRCI + Q technique with Davidson correction. The calculation of the spectroscopic constants and the FCF show the candidacy of the LuF molecule for a direct laser cooling between the two states $X^1\Sigma_{0+}$ and $(1)^3\Pi_{0+}$ with the intermediate state $(1)^3\Delta_1$. Since the influence of this state cannot be ignored, the study of the laser cooling of this molecule has been done by taking into consideration the two transitions $(1)^3\Delta_1$–$(1)^3\Pi_{0+}$ and $X^1\Sigma_{0+} - (1)^3\Pi_{0+}$. Correspondingly, a total branching ratio is investigated with a short radiative time (τ = 3.40 μs) along with the slowing distance, the number of cycles (N) for photon absorption/emission, and the Doppler and recoil temperatures. The time needed to thermalize the molecules in the buffer gas cell is calculated, with the number of collisions in this cell between the molecules with the helium atoms and the mean free path between two collisions. This study of the laser cooling of the molecule LuF paves the way to an experimental laser cooling of this molecule.

Data availability

All data generated or analysed during this study are included in this published article.

Received: 25 May 2022; Accepted: 28 March 2023
Published online: 01 May 2023

References

1. DeMille, D. Quantum computation with trapped polar molecules. *Phys. Rev. Lett.* **88**(6), 067901. https://doi.org/10.1103/PhysRevLett.88.067901 (2002).
2. Lukin, M. D. Colloquium: Trapping and manipulating photon states in atomic ensembles. *Rev. Mod. Phys.* **75**(2), 457–472. https://doi.org/10.1103/RevModPhys.75.457 (2003).
3. Jaksch, D. & Zoller, P. The cold atom Hubbard toolbox. *Ann. Phys.* **315**(1), 52–79. https://doi.org/10.1016/j.aop.2004.09.010 (2005).
4. Micheli, A., Brennen, G. K. & Zoller, P. A toolbox for lattice-spin models with polar molecules. *Nature Phys.* **2**, 5. https://doi.org/10.1038/nphys287 (2006).
5. Ni, K.-K. *et al.* A high phase-space-density gas of polar molecules. *Science* **322**(5899), 231–235. https://doi.org/10.1126/science.1163861 (2008).
6. Baranov, M. A. Theoretical progress in many-body physics with ultracold dipolar gases. *Phys. Rep.* **464**(3), 71–111. https://doi.org/10.1016/j.physrep.2008.04.007 (2008).
7. Carr, L. D., DeMille, D., Krems, R. V. & Ye, J. Cold and ultracold molecules: Science, technology, and applications. *New J. Phys.* **11**(5), 055049. https://doi.org/10.1088/1367-2630/11/5/055049 (2009).

8. Kramer, J. The detection and characterization of the visible emission spectra of lutetium monochloride, monobromide, and monoiodide. *J. Chem. Phys.* **69**(6), 2601–2608. https://doi.org/10.1063/1.436907 (1978).
9. Hamade, Y., Bazzi, H., Sidawi, J., Taher, F. & Monteil, Y. Ab Initio study of the lowest-lying electronic states of LuCl molecules. *J. Phys. Chem. A* **116**(49), 12123–12128. https://doi.org/10.1021/jp305409e (2012).
10. Assaf, J., Taher, F. & Magnier, S. Theoretical description of the low-lying electronic states of LuBr located below 41,700cm−1. *J. Quant. Spectrosc. Radiat. Transfer* **189**, 421–427. https://doi.org/10.1016/j.jqsrt.2016.12.018 (2017).
11. Assaf, J., Taher, F. & Magnier, S. Theoretical investigation of the lowest-lying electronic structure of LuI molecules. *Spectrochim. Acta Part A Mol. Biomol. Spectrosc.* **118**, 1129–1134. https://doi.org/10.1016/j.saa.2013.09.099 (2014).
12. Roederer, I. U., Sneden, C., Lawler, J. E. & Cowan, J. J. New abundance determinations of cadmium, lutetium, and osmium in the process enriched star BD. *ApJL* **714**(1), L123–L127. https://doi.org/10.1088/2041-8205/714/1/L123 (2010).
13. Sneden, C. *et al.* The extremely metal-poor, neutron capture-rich star CS 22892–052: A comprehensive abundance analysis*. *ApJ* **591**(2), 936. https://doi.org/10.1086/375491 (2003).
14. Johnson, J. A. & Bolte, M. The s-process in metal-poor stars: Abundances for 22 neutron-capture elements in CS 31062–050*. *ApJ* **605**(1), 462. https://doi.org/10.1086/382147 (2004).
15. Den Hartog, E. A., Curry, J. J., Wickliffe, M. E. & Lawler, J. E. Spectroscopic data for the 6it s6it p3 P1 level of Lu+ for the determination of the solar lutetium abundance. *Sol. Phys.* **178**, 239–244. https://doi.org/10.1023/A:1005088315480 (1998).
16. Neufeld, D. A., Wolfire, M. G. & Schilke, P. The chemistry of fluorine-bearing molecules in diffuse and dense interstellar gas clouds. *ApJ* **628**(1), 260–274. https://doi.org/10.1086/430663 (2005).
17. Tsuji, T. 1973A&A....23..411T Page 411 (accessed 30 Nov 2022); https://adsabs.harvard.edu/full/1973A&A....23..411T.
18. D'Incan, J., Effantin, C. & Bacis, R. Electronic spectrum of the LuF molecule. *J. Phys. B: Atom. Mol. Phys.* **5**(9), L189–L190. https://doi.org/10.1088/0022-3700/5/9/006 (1972).
19. Effantin, C., Wannous, G., d'Incan, J. & Athenour, C. Rotational analysis of selected bands from the electronic spectrum of the LuF molecule. *Can. J. Phys.* **54**(3), 279–294. https://doi.org/10.1139/p76-033 (1976).
20. Huber, K. *Molecular Spectra and Molecular Structure: IV. Constants of Diatomic Molecules* (Springer Science & Business Media, 2013).
21. Cooke, S. A., Krumrey, C. & Gerry, M. C. L. Pure rotational spectra of LuF and LuCl. *Phys. Chem. Chem. Phys.* **7**(13), 2570–2578. https://doi.org/10.1039/B502683K (2005).
22. Rajamanickam, N. & Narasimhamurthy, B. LuF molecule: True potential energy curve and the dissociation energy. *Acta Phys. Hungar.* **56**(1), 67–71. https://doi.org/10.1007/BF03158017 (1984).
23. Dolg, M. & Stoll, H. Pseudopotential study of the rare earth monohydrides, monoxides and monofluorides. *Theor. Chim. Acta* **75**(5), 369–387. https://doi.org/10.1007/BF00526695 (1989).
24. Jalbout, A. F., Li, X.-H. & Abou-Rachid, H. Analytical potential energy functions and theoretical spectroscopic constants for MX/MX- (M-Ge, Sn, Pb; X-O, S, Se, Te, Po) and LuA (A-H, F) systems: Density functional theory calculations. *Int. J. Quant. Chem.* **107**(3), 522–539. https://doi.org/10.1002/qua.21159 (2007).
25. Shanmugavel, R., Raja, V. & Karthikeyan, B. Evaluation of Franck-Condon factor and R-centroids for some band system of LuF molecule. *Rom. J. Phys.* **54**, 85–92 (2009).
26. Demissie, T. B., Jaszuński, M., Komorovsky, S., Repisky, M. & Ruud, K. Absolute NMR shielding scales and nuclear spin–rotation constants in 175LuX and 197AuX (X = 19F, 35Cl, 79Br and 127I). *J. Chem. Phys.* **143**(16), 164311. https://doi.org/10.1063/1.4934533 (2015).
27. Hamade, Y., Taher, F., Choueib, M. & Monteil, Y. Theoretical electronic investigation of the low-lying electronic states of the LuF molecule. *Can. J. Phys.* **87**(11), 1163–1169. https://doi.org/10.1139/P09-077 (2009).
28. Assaf, J. Étude théorique des molécules LuBr et LuI par les méthodes ab-initio, These de doctorat, Lille 1 (2014). https://www.theses.fr/2014LIL10070.
29. Assaf, J., Zeitoun, S., Safa, A. & Nascimento, E. C. M. Ab-initio study of spin-orbit effect on 175Lu19F spectroscopy. *J. Mol. Struct.* **1178**, 458–466. https://doi.org/10.1016/j.molstruc.2018.10.017 (2019).
30. Werner, H.J., Knowles, P.J., *et al. Molpro, Version 2010.1, a package of ab initio programs* (2022). http://www.molpro.net.
31. Cao, X. & Dolg, M. Segmented contraction scheme for small-core lanthanide pseudopotential basis sets. *J. Mol. Struct. (Theochem)* **581**(1), 139–147. https://doi.org/10.1016/S0166-1280(01)00751-5 (2002).
32. Widmark, P.-O., Malmqvist, P. -Å. & Roos, B. O. Density matrix averaged atomic natural orbital (ANO) basis sets for correlated molecular wave functions. *Theoret. Chim. Acta* **77**(5), 291–306. https://doi.org/10.1007/BF01120130 (1990).
33. Korek, M. A one directional shooting method for the computation of diatomic centrifugal distortion constants. *Comput. Phys. Commun.* **119**(2), 169–178. https://doi.org/10.1016/S0010-4655(98)00180-5 (1999).
34. Korek, M. & El-Kork, N. Solution of the rovibrational schrödinger equation of a molecule using the volterra integral equation. *Adv. Phys. Chem.* **2018**, 1–11. https://doi.org/10.1155/2018/1487982 (2018).
35. Zeid, I., Al-Abdallah, R., El-Kork, N. & Korek, M. Ab-initio calculations of the electronic structure of the alkaline earth hydride anions XH-(X= Mg, Ca, Sr and Ba) toward laser cooling experiment. *Spectrochim. Acta Part A: Mol. Biomol. Spectrosc.* **224**, 117461 (2020).
36. Albert, S., Albert, K. K., Hollenstein, H., Tanner, C. M. & Quack, M. Fundamentals of rotation-vibration spectra. In *Handbook of High-resolution Spectroscopy* (eds Quack, M. & Merkt, F.) hrs003 (Wiley, 2011). https://doi.org/10.1002/9780470749593.hrs003.
37. Hilborn, R. C. Einstein coefficients, cross sections, f values, dipole moments, and all that. *arXiv* https://doi.org/10.48550/arXiv.physics/0202029 (2002).
38. Bernath, P. F. *Spectra of Atoms and Molecules* (Oxford University Press, 2020).
39. Le Roy, R. J. LEVEL: A computer program for solving the radial Schrödinger equation for bound and quasibound levels. *J. Quant. Spectrosc. Radiat. Transfer* **186**, 167–178. https://doi.org/10.1016/j.jqsrt.2016.05.028 (2017).
40. Kang, S.-Y. *et al.* Ab initio study of laser cooling of AlF+ and AlCl+ molecular ions. *J. Phys. B Atom. Mol. Opt. Phys.* **50**, 217. https://doi.org/10.1088/1361-6455/aa6822 (2017).
41. Yuan, X. *et al.* Laser-cooling with an intermediate electronic state: Theoretical prediction on bismuth hydride. *J. Chem. Phys.* **150**, 224305. https://doi.org/10.1063/1.5094367 (2019).
42. Li, R. *et al.* Laser cooling of the SiO+ molecular ion: A theoretical contribution. *Chem. Phys.* **525**, 110412. https://doi.org/10.1016/j.chemphys.2019.110412 (2019).
43. Moussa, A., El-Kork, N. & Korek, M. Laser cooling and electronic structure studies of CaK and its ions CaK$. *New J. Phys.* **23**(1), 013017. https://doi.org/10.1088/1367-2630/abd50d (2021).
44. Moussa, A., El-Kork, N., Zeid, I., Salem, E. & Korek, M. Laser cooling with an intermediate state and electronic structure studies of the molecules CaCs and CaNa. *ACS Omega* **7**(22), 18577–18596. https://doi.org/10.1021/acsomega.2c01224 (2022).
45. Barry, J. F. Laser cooling and slowing of a diatomic molecule, YALE UNIV NEW HAVEN CT (2013).
46. Daniel, J. R. *et al.* Spectroscopy on the transition of buffer-gas-cooled AlCl. *Phys. Rev. A* **104**(1), 012801. https://doi.org/10.1103/PhysRevA.104.012801 (2021).
47. Gantner, T., Koller, M., Wu, X., Rempe, G. & Zeppenfeld, M. Buffer-gas cooling of molecules in the low-density regime: Comparison between simulation and experiment. *J. Phys. B Atom. Mol. Opt. Phys.* **53**, 14. https://doi.org/10.1088/1361-6455/ab8b42 (2020).
48. Iwata, G. Z. A cryogenic buffer-gas cooled beam of barium monohydride for laser slowing, cooling, and trapping. *Columbia Univ.* https://doi.org/10.7916/D8TJ0057 (2018).

Acknowledgements
This publication is based upon work supported by the Khalifa University of Science and Technology under Award No. CIRA-2019-054. Al MESBAR High Power Computer was used for the completion of this work. Faculty: N.E.K is partly supported by the internal grant (8474000336-KU-SPSC).

Author contributions
N.E. Studied and wrote the laser cooling part, A.A. wrote the ab initio part, N.A.E. manuscript revision, J.A. Ab initio calculation with spin-orbit coupling, T.A. Collect the data, E.A. Performed the analysis of the ab initio part, and M.K. Main supervisor and revision of the paper.

Competing interests
The authors declare no competing interests.

Additional information
Correspondence and requests for materials should be addressed to N.E.-K.

Reprints and permissions information is available at www.nature.com/reprints.

Publisher's note Springer Nature remains neutral with regard to jurisdictional claims in published maps and institutional affiliations.